ELECTRONIC CONDUCTIVITY IN $La_{1-x}Ba_xF_{3-x}$ CRYSTALS

A. ROOS and J. SCHOONMAN

Solid State Department, Physics Laboratory, Utrecht University, P.O. Box 80.000, 3508 TA Utrecht, The Netherlands

The electronic conductivities of solid solutions $La_{1-x}Ba_xF_{3-x}$ ($0 < x < 0.0952$) were investigated up to 533 K using the Hebb–Wagner dc polarization technique. The electrochemical cell $(-)$ La|$La_{1-x}Ba_xF_{3-x}$|Pt$(+)$ has been utilized with Pt as the ion-blocking electrode. Under steady-state conditions the $La_{1-x}Ba_xF_{3-x}$ solid solutions exhibit electronic conductivity. The electronic conductivity vanishes in pure LaF_3. Together with ac conductivity measurements it appears that the ionic transference number for $La_{1-x}Ba_xF_{3-x}$ ($0 < x < 0.0952$) is essentially unity over the temperature range studied

1. Introduction

Metal fluorides with the tysonite (LaF_3)-structure exhibit a high conductivity for fluoride ions. Therefore, these materials hold promise for use in electrochemical systems for thermodynamic studies, chemical sensing, and energy conversion and storage.

In fact, the use of LaF_3 as a membrane in thin-film solid state sensors for O_2, CO_2 and NO_2 has been described [1]. Doped with EuF_2 it is the solid membrane in commercial fluoride-ion selective electrodes. Here the membrane is in contact with an aqueous electrolyte which conducts fluoride ions [2]. Applications of metal fluorides in electrochromic systems [3], piezoelectric gauges [4], and infrared detectors [5] have been proposed.

Fluorides with the tysonite structure are assumed to exhibit Schottky disorder, and have electrical properties which are in a number of ways complex. Their reactivity towards oxygen and water vapour appears to interfere strongly in the characterization of the ionic transport. Due to the formation of oxygen-rich surface layers, frequency-dependent effects have been observed. Further, there is still some disagreement concerning the exact lattice structure of LaF_3 [6]. However, a trigonal structure of space-group $P\bar{3}c1$-D_{3d}^4 is the most likely [7]. There are three distinct types of fluoride ion sites in the ratio 12:4:2 (F_1:F_2:F_3). The F_2 and F_3 sites are, however, almost identical in environment and cannot be distinguished in ^{19}F NMR experiments [8].

Early studies of LaF_3 [9,10] have shown large polarization effects and relatively fast ionic motion. The more recent studies on the tysonites [11,12,14] have focused on the ionic conduction mechanism. The ionic conductivity increases only moderately upon doping with BaF_2 [14]. The composition dependence of the ionic conductivity of the anion-deficient solid solutions $La_{1-x}Ba_xF_{3-x}$ reveals a maximum at $\simeq 7$ m/o BaF_2. The localized motions of the solid solutions $La_{1-x}Ba_xF_{3-x}$ have been studied by thermally stimulated depolarization current techniques [15]. The results of these investigations confirm the existence of ion motion in two distinct fluoride ion sublattices.

Usually the application of solid electrolyte materials in practical devices, requires that they exhibit little or no electronic conductivity. As far as we know, the electronic conductivity of tysonite-type solid solutions has never been reported in the literature.

This paper describes the electronic conductivity of LaF_3 and $La_{1-x}Ba_xF_{3-x}$ ($0 \leqslant x \leqslant 0.0952$) crystals as obtained with a polarization technique developed by Hebb [13] and Wagner [16].

2. Hebb–Wagner polarization

The general ideas underlying the polarization

technique to measure electronic conductivity in ionic crystals, and the detailed equations have been discussed by Wagner [16]. Upon application of a potential difference across to the asymmetrical cell $(-)$La$|$La$_{1-x}$Ba$_x$F$_{3-x}|$Pt$(+)$, with the indicated polarity, fluoride ions migrate initially from the La electrode towards the Pt electrode. Under the condition that the applied potential difference E is well below E_d, the decomposition potential of LaF$_3$ ($= 5.811$ V at 298 K), the activities of La, a_{La}, and fluorine, P_{F_2} at the Pt electrode are respectively:

$$a_{La} = a_{La}^0 \exp(-3Eq/kT) , \qquad (1)$$

$$P_{F_2} = a_{La}^{0-2/3} \exp[-2(E_d - E)q/kT] , \qquad (2)$$

where a_{La}^0 is the activity of La at the La$|$La$_{1-x}$Ba$_x$F$_{3-x}$ interface ($a_{La} = 1$), q is the electron charge, k the constant of Boltzmann, and T the absolute temperature. Because no significant fluorine evolution can take place at the Pt electrode for $E \ll E_d$, an excess of fluoride ions will accumulate at this electrode. Under steady-state conditions the migration of fluoride ions due to the electrical field is balanced by diffusion due to the concentration gradient, and the ionic current is completely suppressed. The steady-state current is carried exclusively by electronic charge carriers moving either as electrons or as electron holes. The total electronic current, I, through an ionic conductor with a negative reversible and a positive nonreversible ion-blocking electrode can be expressed by:

$$I = I_e + I_h = kT/qL \{\sigma_e^0[1 - \exp(-qE/kT)]$$

$$+ \sigma_h^0 [\exp(qE/kT) - 1]\} , \qquad (3)$$

where σ_e^0 and σ_h^0 are, respectively, the specific electron and electron hole conductivities in La$_{1-x}$Ba$_x$F$_{3-x}$ in equilibrium with metallic lanthanum ($a_{La} = 1$), and L the cell constant (thickness/area). In the case $\sigma_e^0 \gg \sigma_h^0$ and $qE \gg kT$ the current–voltage curve will show a saturation-current plateau,

$$I_e = (kT/qL) \sigma_e^0 . \qquad (4)$$

With the assumption $\sigma_h^0 \gg \sigma_e^0$, eq. (3) can be reduced to:

$$I_h = (kT/qL) \sigma_h^0 [\exp(Eq/kT) - 1]$$

$$\simeq (kT/qL) \sigma_h^0 \exp(Eq/kT) . \qquad (5)$$

Accordingly, a plot of ln(I) versus E should yield a straight line with a slope of q/kT. σ_h^0 can be obtained from the intercept at $E = 0$.

3. Experimental

The experiments were performed on single crystals of La$_{1-x}$Ba$_x$F$_{3-x}$ ($0 \leqslant x \leqslant 0.0952$) grown by means of a modified Stockbarger crystal growth method. A detailed description of the growth and characterization of the present crystals has been described before [17]. The crystals were measured perpendicular and parallel to the crystallographic c axis. Usually surface areas of $(5-10) \times 10^{-5}$ m^2, and a crystal thickness of $(1-4) \times 10^{-3}$ m were used in the experiments. We started with an asymmetrical polarization cell of the type $(+)$Ni$|$NiF$_2|$La$_{1-x}$Ba$_x$F$_{3-x}|$Pt$(-)$. However, we did not obtain a reversible electrode contact with the Ni$|$NiF$_2$ mixture. The experiments described in this study have been performed with a polarization cell of the type $(-)$La$|$La$_{1-x}$Ba$_x$F$_{3-x}|$Pt$(+)$ using as the reversible electrode a flat disk of lanthanum metal, cut from a lanthanum rod (Koch–Light, nominally 99.9% pure). The ionically blocking Pt electrode is sputtered onto the crystal surface (Edwards S 150, sputter coater). This cell arrangement was clamped between the Pt disk electrodes of a conductivity cell. The La metal and sample handling, were carried out in a glove box, containing an ambient of nitrogen gas. The polarization set-up was placed in this glove box as well. The ambient was purified by means of two BTS (BASF) catalyst traps, and two molecular-sieve traps (Union Carbide), in order to minimize the oxygen and water vapour content.

Measurements were performed in the region from room temperature to 530 K. dc voltages applied to the polarization cells ranged from 0 to 4.5 V, the decomposition voltage of LaF$_3$ being 5.811 V at 298 K. It appears that under potentiostatic conditions the current decreases slowly as a function of time when the measurements were extended over more than a week. This is probably due to inevitable oxygen impurities. The lanthanum cathode was attacked slowly by these impurities, especially at the higher temperatures and voltages. Therefore, the lanthanum disk was grinded after each run. A current–voltage run in the voltage region (2.5–4.5) V lasted usually about one week.

The temperature of the cell was measured with a calibrated chromel—alumel thermocouple. A Keithley digital multimeter (model 191) was used to measure the potential difference across the specimen. Steady-state currents were recorded with an autoranging Keithley picoammeter (model 445), which was commanded by a Solartron data transfer unit (DTU). The DTU transferred time and current data to a tape punch (Facit 4070).

4. Results

Steady-state currents, I, in the cell $(-)La|La_{1-x}Ba_xF_{3-x}|Pt(+)$ ($x = 0.0952$), are presented in fig. 1 as a conductivity IqL/kT versus applied potential difference E. The data recorded at 323 K reveal a plateau between 3.0 and 4.0 V, whereas the curve recorded at 433 K reveals only a shoulder for small potential differences. For higher temperatures plateau currents are completely masked

by a steep increase of the steady-state current with increasing potential difference. According to eq. (4) the plateau conductivity represents the electron conductivity in $La_{1-x}Ba_xF_{3-x}$ ($x = 0.0952$) in equilibrium with the La electrode. Fig. 2 presents the polarization currents in the cell $(-)La|LaF_3|Pt(+)$ versus E. The data reveal electron currents to be negligible in LaF_3 equilibrated with La. Fig. 3 shows the $\ln(IqL/kT)$ versus E plot for this cell arrangement. Straight lines are obtained with a slope of $q/\alpha kT$, with for α values in between 8 and 9. The high-voltage part of the curves presented in fig. 1 reveals a similar deviation from the Wagner theory of polarization.

The electron conductivities of the studied solid solutions $La_{1-x}Ba_xF_{3-x}$ are gathered in table 1. The electronic conductivities of these materials reveal no anisotropy. The compositions of the $La_{1-x}Ba_xF_{3-x}$ samples reported here, have been determined by neutron activation analysis [14], and are included in table 1 The unblocked specific ionic current of these materials, has been reported in a previous study [14]. These data
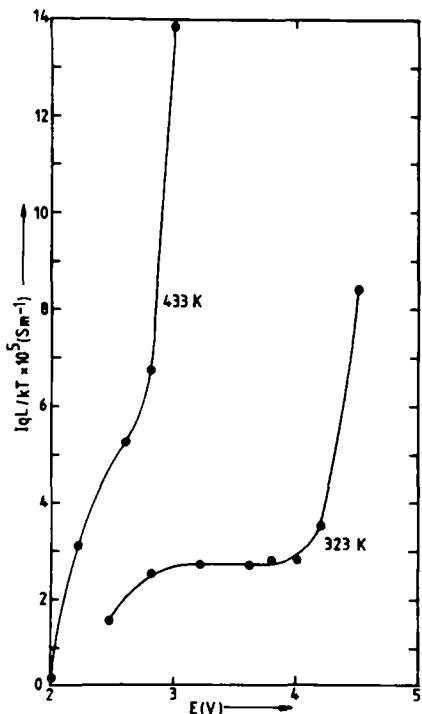

Fig. 1. Steady-state polarization current ($\perp c$ axis), plotted as IqL/kT versus E in the cell $(-)La|La_{1-x}Ba_xF_{3-x}|Pt(+)$ ($x = 0.0952$) at 323 and 433 K, $L = 281$ m^{-1}.
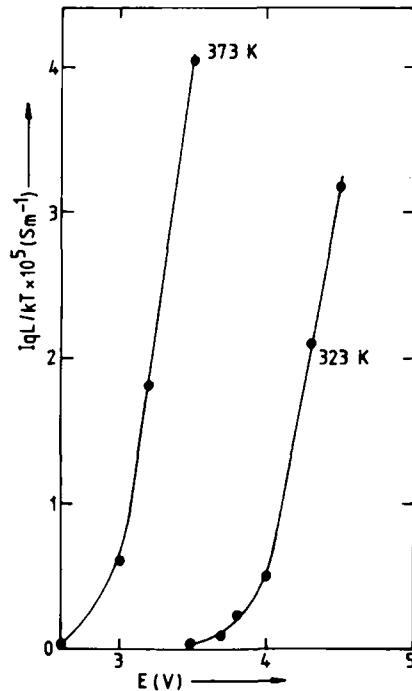
Fig. 2. Steady-state polarization current ($\perp c$ axis), plotted as IqL/kT versus E in the cell $(-)La|LaF_3|Pt(+)$ at 323 K and 433 K, $L = 147$ m^{-1}.
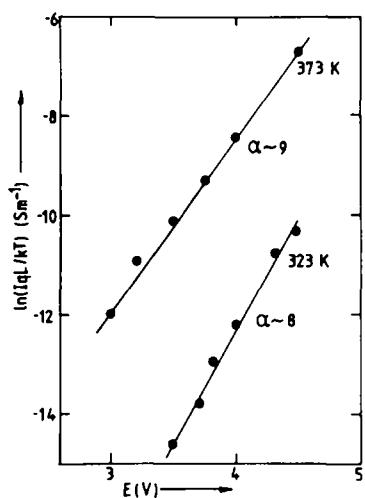
Fig. 3. Steady-state polarization current for the cell $(-)$La|LaF$_3$|Pt$(+)$, presented as $\ln(IqL/kT)$ versus E (see text).

reveal that the contribution of the electronic current to the total conductivity is negligible. For comparison the ionic conductivity data of the samples have also been included in table 1. The conductivity is primarily ionic so that the equilibrium electronic transference number,

$$t_e^0 = \sigma_e^0/(\sigma_i + \sigma_e^0) \simeq \sigma_e^0/\sigma_i \ll 1 \qquad (6)$$

hence $IqL/kT = \sigma_e^0 = t_e^0\sigma_i$. Values for t_e^0 are included in table 1. The data in table 1 reveal a tendency for t_e^0 to decrease with increasing solute content.

5. Discussion

The present results indicate that the solid solutions $La_{1-x}Ba_xF_{3-x}$ exhibit excess electron conduction when equilibrated with La metal. The transference numbers indicate that the deviations from stoichiometry are extremely small. The electronic conductivity in LaF$_3$ cannot be measured.

With regard to the polarization cell $(-)$La|La$_{1-x}$Ba$_x$F$_{3-x}$|Pt$(+)$, the equilibrium between the solid electrolyte and the cathode can be expressed, using the assumption that the thermal defects in LaF$_3$ are generated according to a Schottky mechanism:

$$La(S) \rightleftharpoons La_{La}^X + 3V_F^{\cdot} + 3e' ,$$
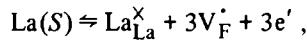
$$k_{La} = [V_F^{\cdot}]^3[e']^3/a_{La} . \qquad (7)$$

Here, the defect notation of Kröger is used [23]. k_{La} represents the equilibrium constant, while $a_{La} = 1$. Divalent barium ions at lanthanum ion sites, Ba$_{La}'$, require fluoride ion vacancies for charge decomposition:

$$BaF_2 \rightarrow Ba_{La}' + V_F^{\cdot} + 2F_F^X . \qquad (8)$$
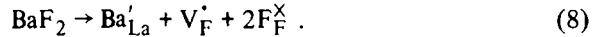
With regard to the present results one can use a reduced electroneutrality condition for the extrinsic region of the anion-deficient solid solutions, i.e.

$$[e'] + [Ba_{La}'] = [V_F^{\cdot}] . \qquad (9)$$

From this relation we obtain with the equilibrium constant k_{La} and eq. (8) for the electron concentration:

$$[e'] = \tfrac{1}{2}([BaF_2]^2 + 4k_{La}^{1/3})^{1/2} - \tfrac{1}{2}[BaF_2] . \qquad (10)$$

This relation shows that the electron concentration

Table 1
Composition parameter x, electron (σ_e^0) and ionic (σ_i) conductivity (Sm^{-1}) and transference numbers (t_e^0) of the studied solid solutions La$_{1-x}$Ba$_x$F$_{3-x}$ at 3 temperatures: $T_1 = 323$ K, $T_2 = 373$ K, $T_3 = 433$ K.

	x (m/o)	σ_e^0	σ_i	t_e^0
T$_1$	1.30	$(2.8 \pm 0.4) \times 10^{-5}$	9.8×10^{-3}	2.9×10^{-3}
	9.52	$(2.8 \pm 0.4) \times 10^{-5}$	1.7×10^{-2}	1.6×10^{-3}
T$_2$	1.30	$(1.0 \pm 0.1) \times 10^{-4}$	4.2×10^{-2}	2.4×10^{-3}
	9.52	$(2.7 \pm 0.4) \times 10^{-5}$	7.6×10^{-2}	3.6×10^{-4}
T$_3$	1.30	—	—	—
	9.52	$(5.2 \pm 0.7) \times 10^{-5}$	3.3×10^{-1}	1.6×10^{-4}

decreases upon doping with barium fluoride and vanishes for $[BaF_2]^2 \gg 4k_{La}^{1/3}$. Considering eq. (10) one would expect the electron conductivity in LaF_3 in equilibrium with La to exceed that in the anion-deficient solid solutions. However, plateau currents could not be observed in the current–voltage characteristics of the undoped materials. A predominant electron hole conductivity seems not likely, because the $\ln(IqL/kT)$ versus E plot for nominally pure LaF_3 (fig. 3) exhibits a slope $q/\alpha kT$ with a value of about 8 for α. This α value deviates substantially from Wagner's theory, which predicts for α the value one. The polarization current–voltage characteristics of the anion-deficient solid solutions (fig. 1) also reveal values of α which are much larger than one. Such a large value of α has been observed many times before and has, amongst others, been ascribed to partial blocking of the ionic current [21,25]. Brook et al. [24] have considered a relaxed requirement of complete blocking of ions at the inert interface, in that a residual ionic current I_{ir} is allowed for. This requirement is valid under the condition that $I_{ir} \ll I_{io}$, the ionic current in the absence of polarization. With this assumption eq. (5) becomes:

$$I_h = \frac{kT}{qL} \sigma_h^0 \{\exp[(1 - I_{ir}/I_{io}) qE/kT] - 1\} . \quad (11)$$

If we further assume I_{ir} to be voltage invariant over a large range of E, while $I_{io} = E/R_{io}A$, A being the electrode area and R_{io} the corresponding ionic resistance, we obtain for large E:

$$\ln I_h = \{\ln[(kT/qL) \sigma_h^0] - qI_{ir}R_{io}A/kT\} + qE/kT . \quad (12)$$

From this expression we see that the correction term goes in the intercept, contrary to the present observations, and consequently showing I_{ir} to be a function of the applied potential difference. This indicates ionic contributions governed by eq. (2) to be dominant over the electron hole contribution. Decomposition is especially obvious from the high-temperature data ($T > 530$ K) and relatively large applied potential differences.

In order to account for large α values Joshi and Liang [25] have proposed for cells $(-)Pb|PbF_2|C(+)$, that eq. (3) is only valid if the ionic conductivity (σ_i) is much larger than the electronic conductivity σ_e. For a positive blocking electrode on LaF_3 the elec-

tron hole concentration, and hence σ_h, is highest at the $LaF_3|Pt$ interface, where LaF_3 interacts with fluorine according to

$$\tfrac{1}{2}F_2 + V_F^{\cdot} \leftrightharpoons F_F^X + h^{\cdot} . \quad (13)$$
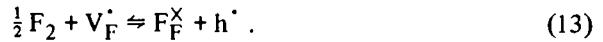
With eq. (2) and the condition $\sigma_i \gg \sigma_e$ we can in principle find an expression for a critical potential E_c. It has recently been shown, however, that the constraint $\sigma_i \gg \sigma_e$ is far too severe [20], because eq. (3) is valid only if the concentration of the ionic point defects is constant over the whole range of chemical potential of metal or non-metal covered by the applied potential; i.e. the deviations from stoichiometry remain small. In addition electronic defect mobilities are usually much larger than ionic defect mobilities, so we may have $\sigma_e > \sigma_i$ for small deviations from stoichiometry. With a concentration constraint $[h^{\cdot}] \lesssim 0.01 \,]V_F^{\cdot}]$ one obtains eq. (3) to be valid if [20]:

$$\sigma_h^0/\sigma_i < 10^{-2} \mu_h^{\cdot}/\mu_{V_F^{\cdot}} , \quad (14)$$

where $\mu_h^{\cdot}$ and $\mu_{V_F^{\cdot}}$ are the electron hole and the anion vacancy mobility, respectively. We have determined only ionic defect mobilities (see ref. [14]) so we cannot present a more specific value for the constraint. However, in the limiting case, $[h^{\cdot}] = [V_F^{\cdot}]$, one would expect $\alpha = 2$, ref. [23]. We are, therefore, lead to the conclusion that partial blocking of the ionic current at the $LaF_3|Pt$ interface is the main origin of the present deviations from the Wagner theory.

A negligible electron current in nominally pure LaF_3 may be caused by a residual cerium impurity. In previous studies [15,17] we have demonstrated that Ce is present as a minor residual impurity in the starting LaF_3 materials used here. The presence of Ce^{4+} in tysonite $(La,Ce)F_3$ has been reported in the literature [18]. CeF_4 is compensated by lanthanum vacancies

$$3 CeF_4 \rightarrow 3 Ce_F^{\cdot} + V_{La}''' + 12F_F^X . \quad (15)$$
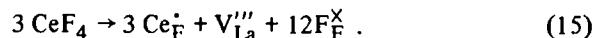
For CeF_4-doped LaF_3 we can use the electroneutrality condition:

$$[e'] + 3[V_{La}'''] = [Ce_{La}^{\cdot}] . \quad (16)$$

With $k_s = [V_{La}'''] [V_F^{\cdot}]^3$ and eq. (7) we obtain:

$$k_{La} = k_s/[V_{La}'''] [e']^3 , \quad (17)$$

and substituting this equation into eq. (16) yields:

$$3[e']^3 k_s/k_{La} + [e'] - [Ce_{La}^{\cdot}] = 0 . \tag{18}$$

Solving eq. (18) we obtain a cumbersome equation for $[e']$, which will not be presented here as this will not be used in a quantitative analysis. This relation shows that in principle the electron concentration would increase with increasing amount of CeF_4. However, Ce^{4+} ions have been reported also to act as an electron trap (19), thereby reducing $[e']$ if CeF_4 contaminated LaF_3 is equilibrated with La. When LaF_3 is doped with BaF_2, eq. (8), Ba_{La}' ions will initially compensate the $Ce_{La}^{\cdot}$ ions, thereby reducing the V_{La}''' concentration and hence the electron concentration. In this way our observations can be understood qualitatively.

As mentioned before, the polarization currents decrease during prolonged potentiostatic measurements. This decrease can be ascribed to the incorporation of inevitable residual oxygen into the LaF_3 lattice, according to:

$$\tfrac{1}{2}O_2 + 2F_F^X \rightleftharpoons V_F^{\cdot} + O_F' + F_2 \tag{19}$$

or

$$\tfrac{1}{2}O_2 + V_F^{\cdot} \rightleftharpoons O_F' + 2h^{\cdot} . \tag{20}$$
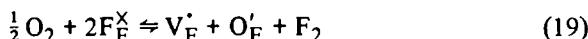
The former lattice reaction reveals oxygen to exert a similar influence on $[e']$ as anticipated for BaF_2. Both types of impurities increase the concentration of fluoride ion vacancies, and according to eq. (10) reduce the electron concentration. The latter reaction would initially lead to a decrease, but eventually to an increase of the polarization currents in time.

We can conclude that in the temperature region (323–433) K conduction by electrons, rather than by electron holes, is predominant in anion-deficient solid solutions $La_{1-x}Ba_xF_{3-x}$ in equilibrium with La. As outlined before by Kennedy [22], the value for the specific electron conductivity σ_e^0 represents the highest possible value for the electronic conductivity, because this value refers to the electronic conductivity which would be observed in the cell $La|La_{1-x}Ba_xF_{3-x}|La$. At high applied potential differences the observed polarization currents were not reproducible, probably due to partial blocking of the ionic current at the inert interface.

We can estimate the voltage region in which the studied cells can be used. These cells reveal an open-circuit potential $(V_{o.c.})$ of about 2.4 V at 323 K. In general, cells are not operated at voltages lower than the maximum powerpoint $(V_{o.c.}/2 = 1.2\ V)$ assuming no other polarization losses. Kennedy [22] has proposed to quote an "electronic decomposition potential" for electronic conductors. The current-potential curve is similar in nature to an electrochemical decomposition curve, and an extrapolation back to zero current would be a helpful potential to quote. Fig. 1 (curve for 323 K) indicates an electronic decomposition potential of about 4.0 V at 323 K. We conclude that the electrochemical cells described in this paper, can be used in the voltage region (1.2–4.0) V.

Acknowledgement

References

[1] B.C. LaRoy, A.C. Lilly and C.O. Tiller, J. Electrochem. Soc. 120 (1973) 1668.

[2] M. Frant and J. Ross, Science 154 (1966) 1553.

[3] C.E. Rice and P.M. Briderbaugh, Appl. Phys. Letters 38 (1981) 59.

[4] S. Matar, J.M. Réau, G. Demazeau, C. Lucat, J. Poitier and P. Hagenmuller, Solid State Commun. 35 (1980) 681.

[5] A. Sher, C.L. Fales and J.F. Stubblefield, Appl. Phys. Letters 28 (1976) 676.

[6] Gmelin Handbuch der Anorganischen Chemie, Seltenerdelemente, Teil C3, Sc, Y, La und Lanthanide, 8th Ed. (Springer, Berlin, 1976) pp. 50–60.

[7] B. Maximov and H. Schulz, Acta Cryst. B., to be published.

[8] A.F. Aalders, A. Polman, A.F.M. Arts and H.W. de Wijn, Solid State Ionics 9/10 (1983) 539.

[9] A. Sher, R. Solomon, K. Lee and M.W. Muller, Phys. Rev. B144 (1966) 593.

[10] M. Goldman and L. Shen, Phys. Rev. B144 (1966) 321.

[11] A.V. Chadwick, D.S. Hope, G. Jaroszkiewicz and J.H. Strange, in: Fast ion transport in solids, eds. P. Vashishta, J.N. Mundy and G.K. Shenoy (North-Holland, Amsterdam, 1979) p. 683.

[12] J. Schoonman, G. Oversluizen and K.E.D. Wapenaar, Solid State Ionics 1 (1980) 211.

[13] M.H. Hebb, J. Chem. Phys. 20 (1952) 185.

[14] A. Roos, F.C.M. van de Pol, R. Keim and J. Schoonman, Solid State Ionics 13 (1984) 191.

[15] A. Roos, M. Buijs, K.E.D. Wapenaar and J. Schoonman, J. Phys. Chem. Solids, to be published.
[16] C. Wagner, Z. Electrochem. 60 (1956) 4.
[17] A. Roos, Mat. Res. Bull. 18 (1983) 405.
[18] Gmelin Handbuch der Anorganischen Chemie, Seltenerdelemente, Teil C3. Sc, Y, La und Lanthanide, 8th Ed. (Springer, Berlin, 1976) pp. 184–186.
[19] H.H. Fujimoto and H.L. Tuller, in: Fast ion transport in solids, eds. P. Vashishta, J.N. Mundy and G.K. Shenoy (North-Holland, Amsterdam, 1979) p. 649.

[20] J. Schoonman, A. Wolfert and D.F. Untereker, Solid State Ionics 11 (1983) 187.
[21] A.R. Lingras and G. Simkovich, J. Phys. Chem. Solids 39 (1978) 1225
[22] J.H. Kennedy, J. Electrochem. Soc. 124 (1977) 865.
[23] F.A. Kröger, The chemistry of imperfect crystals, 2nd Rev. Ed., Vol. 2 (North-Holland, Amsterdam, 1974).
[24] R.J. Brook, W.L. Pelzmann and F.A. Kröger, J. Electrochem. Soc. 118 (1971) 185.
[25] A.V. Joshi and C.C. Liang, J. Phys. Chem. Solids 36 (1975) 927.